MOLECULAR PHYSICS, 1990, VOL. 71, NO. 5, 1143–1153

Photofragment orientation as a probe of near-threshold non-adiabatic phenomena in the photodissociation of ICN

By J. F. BLACK†, E. HASSELBRINK‡, J. R. WALDECK§ and R. N. ZARE
Department of Chemistry, Stanford University, Stanford, California 94305, U.S.A.

(*Received 18 May 1990; accepted 14 June 1990*)

Cyanogen iodide (ICN) is photodissociated at 249 nm. The CN($X\,^2\Sigma^+$, $v = 2$) fragments are probed by sub-Doppler laser-induced fluorescence (LIF) using circularly polarized light, which allows resolution of the $F_1(J = N + \frac{1}{2})$ and $F_2(J = N - \frac{1}{2})$ spin–rotation doublets. These components are shown to be oriented, i.e. to possess a non-statistical non-centrosymmetric M_J quantum-state distribution. The sign and magnitude of the orientation vary between components and are shown to have some correlation with the energetic threshold for production of the $I(^2P_{1/2})$ spin–orbit state. These observations are briefly discussed in the context of breakdown of the Born–Oppenheimer approximation in this system.

1. Introduction

The science of photochemistry has advanced steadily from simple beginnings (see e.g. Scheele's 1777 study of the darkening of silver chloride with violet light [1]) to probing the most fundamental properties of molecular dissociation [2, 3]. Of particular interest are current efforts to use the vector and coherence properties of laser light to obtain a microscopic understanding of molecular structure and dynamics [4, 5]. This paper describes an experimental study of one such phenomenon, namely the intimate coupling of photon angular momentum with molecular reaction dynamics. Vasyutinskii [6] photodissociated caesium iodide with circularly polarized light and, using a magnetic resonance/circular dichroism technique, observed that the $Cs(^2S)$ atoms were *oriented*. By orientation, we mean a non-statistical distribution of M_J levels, with the population of positive M_J values not equal to that of negative M_J values. In a follow-up investigation [7], Vasyutinskii further noted that the sign of the macroscopic orientation differed, depending on whether the $Cs(^2S)$ was produced in conjunction with $I(^2P_{1/2})$ or $I(^2P_{3/2})$. This selectivity was achieved by varying the energy of the photodissociating light.

Vasyutinskii's work was the first study to confirm a direct link between photon helicity and angular momentum coupling in *molecular dissociation*. The phenomenon of producing spin-polarized electrons by photoionizing atoms with circularly polarized light has been known for some time in the atomic-physics community [8–10], but the extension to molecules has seldom been made. Recently, Hasselbrink *et al.* [11]

† Present address: Continuum, 3150 Central Expressway, Santa Clara, California 95051, U.S.A.

‡ Present address: Fritz-Haber-Institüt der Max-Planck Gesellschaft, Faradayweg 4-6, 1000 Berlin 33, Federal Republic of Germany.

§ Present address: Department of Chemistry, University of Pittsburgh, Pittsburgh, Pennsylvania 15260, U.S.A.

0026-8976/90 $3.00

photodissociated ICN with circularly polarized light at 249 nm, in the heart of what is called the 'Ã continuum' (see [12] for a recent analysis of photodissociation at this wavelength). In analogy to the experiments of Vasyutinskii, this study found that the rotational angular momenta of the $CN(X\,^2\Sigma^+, v = 0, N)$ fragments were strongly oriented and the sign of the orientation was directly correlated with the spin–orbit state of the iodine atom partner. (Black *et al.* [13] have also shown this correlation.)

Vigué *et al.* [14] have proposed a theoretical model for the observed orientation, invoking a coherent superposition of parallel and perpendicular electronic transitions in the initial photon absorption and subsequent vibronic angular-momentum 'amplification'. This phenomenon has also been discussed by Dixon [15] for the photodissociation of NH_3.

Hasselbrink *et al.* [11] also probed the $CN(X\,^2\Sigma^+, v = 2, N)$ manifold over a spectroscopically isolated and uncongested range of N. They made the subtle observation that when the F_1 and F_2 spin–rotation doublets of the $X\,^2\Sigma^+$ state were unresolved, there was no observable orientation, but when these components were spectroscopically resolved, they exhibited orientation of roughly equal magnitude but *opposite* sign. This observation appears to be outside the realm of the Vigué theory, and we must look elsewhere for the explanation.

In 1981, Freed and co-workers published the first two members [16, 17] of a series of papers [18] describing the photodissociation of diatomic molecules in which the dissociation yielded open-shell fragments, i.e. fragments with non-vanishing electronic angular momentum. The essence of the theory was that the Born–Oppenheimer approximation would necessarily break down under conditions yielding open-shell fragments. The theory predicts a wide range of subtle non-adiabatic effects in cases of near-threshold photodissociation, but, to date, we are not aware of any experimental confirmations of these phenomena.

We have studied the photodissociation reaction

$$ICN + h\nu(249\,nm) \rightarrow I(^2P_{1/2}, {}^2P_{3/2}) + CN(X\,^2\Sigma^+, v, N).$$

This dissociation is one of the most thoroughly investigated contemporary systems, but nevertheless remains poorly understood at any level of discussion [12]. There is an increasing body of evidence suggesting that non-adiabatic forces, acting in the dissociation, produce anomalies in the fragment quantum-state population distributions, angular distributions, orientation and alignment.

In this paper we build on the results of Hasselbrink *et al.* [11] by examining the $v = 2$ manifold with high-resolution Doppler-limited spectroscopy [13, 19]. Our results, cross-correlated with the other existing evidence, provide experimental confirmation of the theories of Band, Freed, Kouri, Singer and co-workers. We shall also briefly discuss the origins of the phenomena.

2. Experimental

The experimental design philosophy and implementation have been discussed extensively elsewhere [11–13, 19–21]. The only fundamental change from the work of Hasselbrink *et al.* [11] is the position of the photoelastic modulator (PEM) (HINDS, CF4 head), which is now placed to modulate the polarization of the photolysis beam. Figure 1 shows the present experimental arrangement.

Briefly, 249 nm light from an excimer laser (Lumonics TE860-2) provided both the photolysis photons and the pump source for a dye laser (Lambda Physik FL2002E). The photolysis laser beam was first linearly polarized, recollimated, and then sent

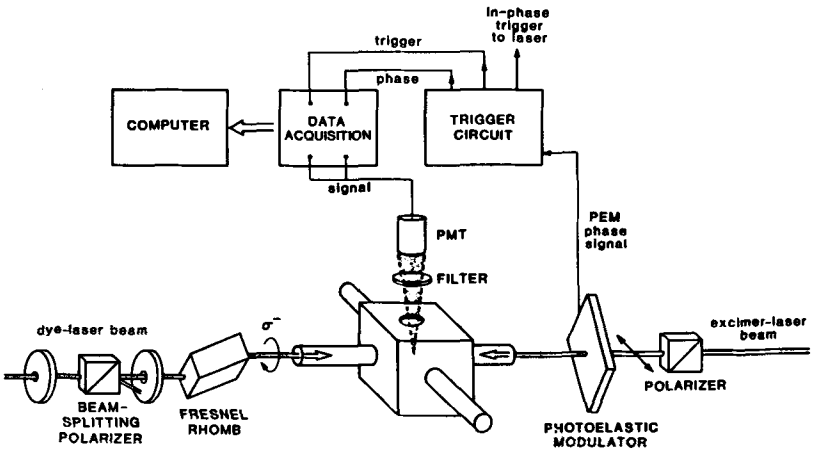

Figure 1. Schematic diagram of the apparatus used in the orientation experiments.

through the crystal of the PEM. The compression amplitude of the PEM was adjusted to give $\pm\frac{1}{4}\lambda$ retardation at 249 nm, yielding left- and right-handed circularly polarized light on alternate laser shots. This beam was then directed into the vacuum chamber via extensively baffled arms, which were purged with argon (10 mTorr). The photolysis laser power in the interactions zone was always less than 750 μJ.

The dye laser produced probe radiation at around 460 nm (Coumarin 450 in methanol, Exciton) in a bandwidth of $\leqslant 0{\cdot}06\,\mathrm{cm}^{-1}$ (with an intracavity etalon). This wavelength is resonant with the (0, 2) transition in the CN $B^2\Sigma^+$–$X^2\Sigma^+$ system [22–27]. The dye-laser beam was first linearly polarized and then sent into a Fresnel rhomb (Karl Lambrecht FR2-272-UN). This produced light of one helicity only, which was directed into the vacuum chamber counterpropagating to the photolysis beam. An optical delay line provided a 35 ns delay between the pump and probe pulses. Great care was taken to preserve the purity of the helicities of the two beams, including nulling out stress-induced birefringence in optical components in the beam paths. The dye-laser power used was 4 μJ per pulse. For the doubly off-diagonal transition probed in this study, this value is well below the calculated saturation onset.

Fluorescence was viewed by a lens (f = 60 mm) mounted inside the vacuum chamber and focused onto the photocathode of a photomultiplier tube (PMT) (RCA 7326, 1700 V bias). We observed the (0, 0) band through an interference filter (Omega Optical) centred on the $\Delta v = 0$ sequence at around 385 nm. The PMT signal was amplified (LeCroy VV100BTB) and then integrated for 120 ns (SRS 250 boxcar). The analog output was digitized in a laboratory microcomputer, which also performed a simple channel separation based on the compression cycle of the PEM. This variation on the technique of Hasselbrink *et al.* [11] was found to produce line-integrated results identical with those of that work. The present method has already been used to probe the CN($v = 0$) fragments from the photodissociation of ICN at 249 nm in a sub-Doppler fashion [13].

ICN (Kodak) was sublimed *in vacuo* and then allowed to flow through the chamber at pressures of 2–10 mTorr. There was no evidence for collisional quenching or memory effects from previous laser pulses at this pressure.

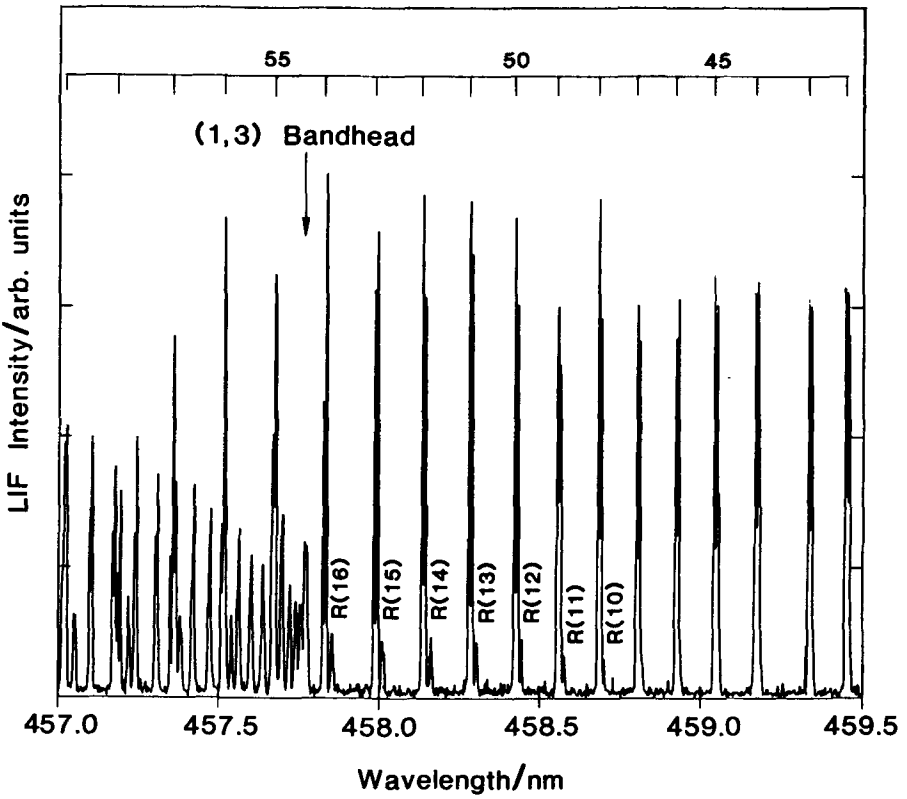

Figure 2. Laser-induced fluorescence spectrum of the CN $B^2\Sigma^+$–$X^2\Sigma^+$ (0, 2) band in the region studied here. The major progression is the P branch of the (0, 2) band, with the R branch and (1, 3) bandhead also appearing.

3. Results

Figure 2 shows a portion of the CN $B^2\Sigma^+$–$X^2\Sigma^+$ (0, 2) band system, in this case taken under broadband (no etalon) probe-laser conditions. The major progression is the high-N part of the P branch. This branch rapidly converges to a bandhead at lower wavelengths. From $N = 10$ onwards, members of the R branch start to appear, initially as small satellites on the more intense P-branch lines. The secondary feature at 457·8 nm is the (1, 3) P-branch bandhead. At shorter wavelengths we observe additionally the (2, 4) and (3, 5) bandheads.

The prominent P lines of the (0, 2) progression appear to be structured. This is caused by spin–rotation doubling of each N level into two J levels. The relatively broad bandwidth for the conditions of this spectrum (0·12 cm^{-1}) permits only partial resolution of these doublets. In this geometry, the line profiles are relatively insensitive to the translational energy imparted into the fragments in the dissociation [12]. This is, however, the preferred geometry in which we perform experiments with circularly polarized light to yield information on the *odd* moments of the angular-momentum distribution [11, 13].

Figure 3 (*a*) shows a sub-Doppler scan over the P(37) line of the CN B–X (0, 2) band. The two peaks are the F_1 and F_2 spin–rotation doublets. The solid line denotes the area where the helicities of the pump and probe photons are the same, while the

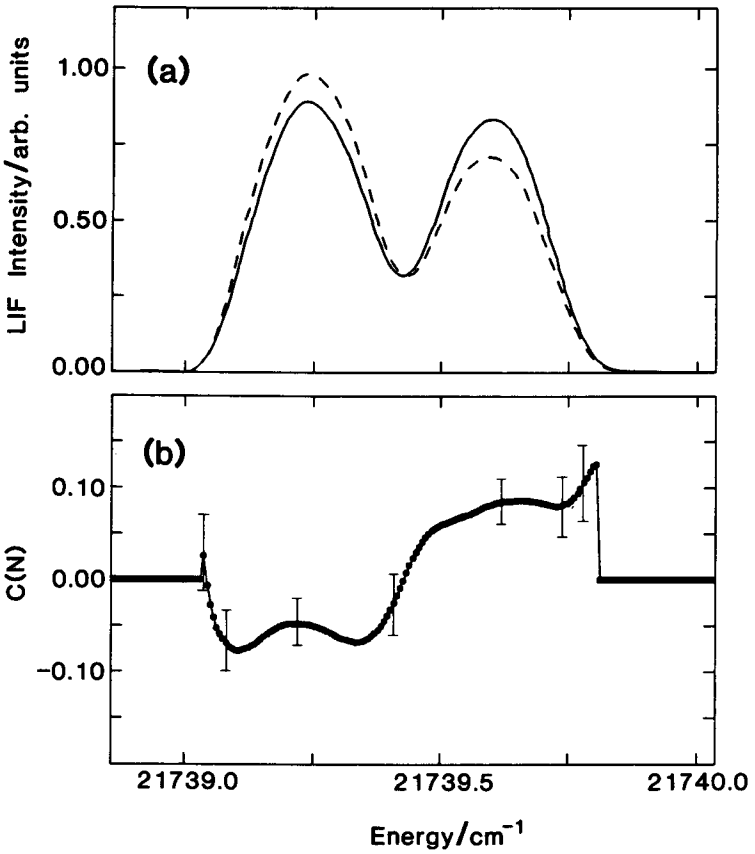

Figure 3. High-resolution LIF signal from P(37), (*a*), and the resulting orientation function $C(37)$, (*b*). Errors are 2σ, propagated from the raw LIF spectrum data. Energies are in vacuum wavenumbers.

dashed line denotes opposite helicites. The data used to create this plot and those of figure 5 have been smoothed by folding with a Gaussian function calculated to have the same width as the laser linewidth. We see that the F_1 and F_2 components exhibit different responses to the relative helicities of the the photon fields, confirming the remarkable original result of Hasselbrink *et al.* [11]. We define the degree of circular polarization $C(N)$ as

$$C(N) = \frac{I_{\uparrow\uparrow}(N) - I_{\uparrow\downarrow}(N)}{I_{\uparrow\uparrow}(N) + I_{\uparrow\downarrow}(N)}. \tag{1}$$

Figure 3 (*b*) shows a plot of $C(37)$, extracted from the data of figure 3 (*a*) and displayed as a function of the probe-laser frequency (vacuum wavenumbers). We see that the fine-structure components have roughly the *same* magnitude of orientation but *oppposite* sign. The thick line is the difference-over-sum function from the smoothed data, whereas the error bars (2σ) are calculated by propagation from the raw, unsmoothed experimental data. Note that the error in the difference-over-sum construction of (1) is sensitive to the absolute magnitude of the signals being compared. One result of this is an increased error in the wings of the Doppler profiles.

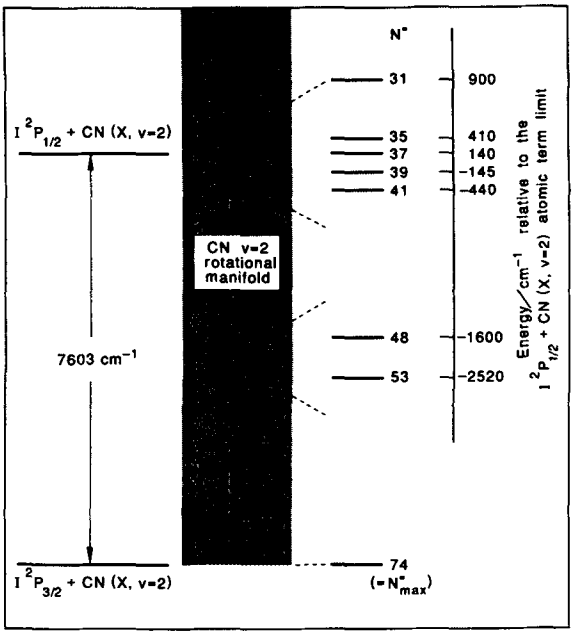

Figure 4. Schematic diagram of the CN ($X\,^2\Sigma^+$, $v = 2$, N) level stack, showing the positions of the rotational levels relative to the I-atom term limits and the positions of the lines studied.

In this study we have analysed a similar range of N as Hasselbrink *et al.* [11]. Figure 4 shows a plot of the level structure in energy space. The CN ($X\,^2\Sigma^+$, $v = 2$) rotational-level 'stack' is shown inverted, in that the energy difference between a rotational level and one or the other iodine atomic-term limits corresponds to the energy remaining for translation with that particular atomic-fragment partner. The positions of the levels in the stack, relative to the ordinate, were calculated from our previous determination of the system energetics at this photolysis wavelength. At these values of N the error in the available energy ($14\,400 \pm 200\,\text{cm}^{-1}$ [12]) corresponds to an error in fixing N to the atomic-term thresholds of ± 1 quantum.

Figure 5 shows the observed $C(N)$ function for six lines: P(31), P(35), P(39), P(41), P(48) and P(53). Complete resolution of the fine-structure components is achieved by P(48). We see that the degree-of-orientation function $C(N)$ for the five lines clustered around the $I(^2P_{1/2})$ atomic-term threshold exhibits similar behaviour in that the fine-structure components show response of roughly equal magnitude but opposite sign. This is in accord with the observations of Hasselbrink *et al.* [11]. The two lines, P(48) and P(53), that are well removed from the $I(^2P_{1/2})$ term limit exhibit different behaviour, however. For these two lines the degree of orientation now shows dissimilar magnitude and identical sign. The sign of the orientation for these two components is the same as that for the CN ($X\,^2\Sigma^+$, $v = 0$, N) lines already correlated with the $I(^2P_{3/2})$ term limit.

For all the lines studied there is no significant change in $C(N)$ over the Doppler profile of each fine-structure component, indicating that, to within our present experimental error limits, there seems to be no velocity–angular-momentum correlation inherent in the results.

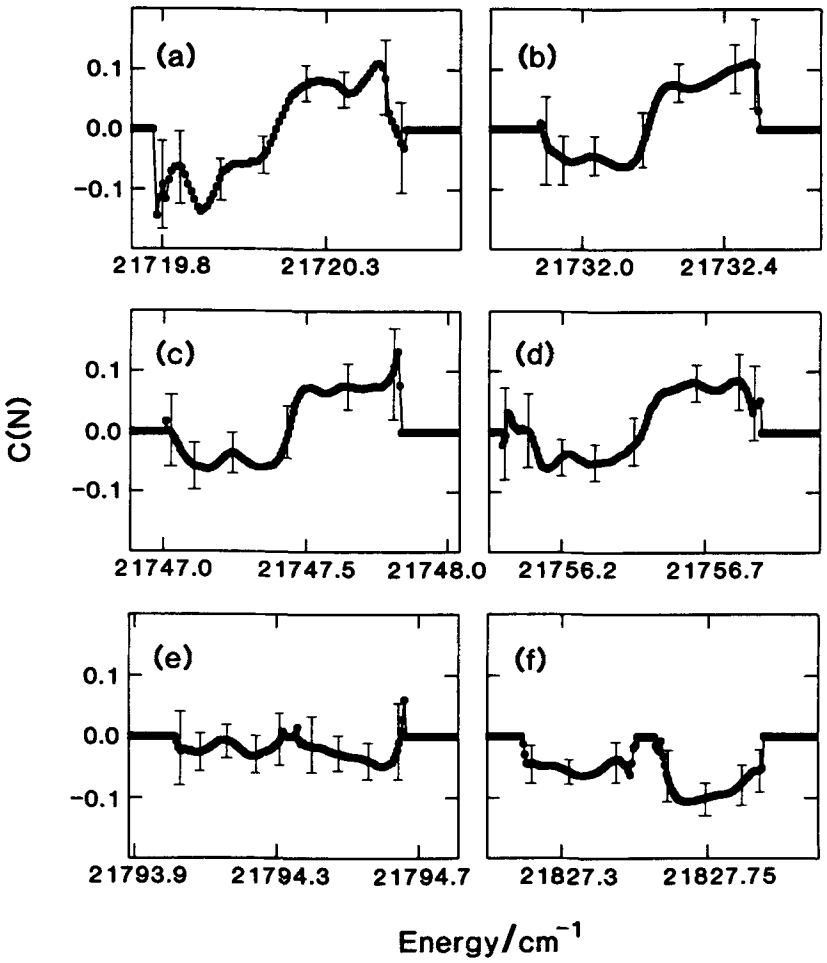

Figure 5. Orientation functions for (*a*) P(31), (*b*) P(35), (*c*) P(39), (*d*) P(41), (*e*) P(48) and (*f*) P(53) lines. Note the change in appearance of the profiles. Error bars are 2σ, propagated from the raw LIF spectral data. Energies are in vacuum wavenumbers.

4. Discussion

Previous analyses of the properties of the CN $X^2\Sigma^+$ fragments from the photodissociation of ICN at 249 nm have established the following:

(*a*) the F_1 and F_2 fine-structure components in the $v = 0$ and $v = 2$ manifolds are non-statistically populated [12, 21];

(*b*) the F_1 and F_2 components in the $v = 0$ manifold have different angular distributions [12, 28, 29];

(*c*) the F_1 and F_2 components in the $v = 0$ manifold have different alignments (in that the quadrupole moments of the spatial angular momentum distributions of the two fine-structure components are different) [19, 28, 29];

(*d*) the rotational angular momenta of the CN fragments are oriented when ICN is photodissociated with circularly polarized light [11, 13], with the sign of orientation correlated with the iodine-atom spin–orbit state.

In this work (extending that of Hasselbrink *et al.*), we observe that the F_1 and F_2 components have different orientations (in that the dipole moment of the spatial angular-momentum distribution is different between the two levels). Furthermore, there seems to be a correlation between the sign and degree of the orientation and the proximity of one of the atomic-partner term thresholds. Referring to the 'checklist' of Band *et al.* [16, 17], we note that all but one of the listed features, signifying the action of non-adiabatic interactions, have now been observed for this system. To date, we have made no observation of a velocity correlation with the orientation, but experience suggests that this will be a very subtle effect and difficult to isolate.

To the best of our knowledge, this is the first compelling data set validating the original predictions of the theory of Band, Freed, Kouri, Singer and co-workers [18]. We discuss briefly the origins of non-adiabatic phenomena in this type of system, following the original precepts derived for diatomic dissociation.

The dissociation

$$\mathrm{ICN} + h\nu(249\,\mathrm{nm}) \rightarrow \mathrm{I}(^2\mathrm{P}) + \mathrm{CN}(^2\Sigma^+)$$

is now known to involve at least three interacting potential-energy surfaces [12]. The absolute electronic nature of the continuum is presently unclear, but is likely to be described as either a $\pi^3\pi$ or $\pi^3\sigma$ molecular-orbital configuration [30, 31]. Under (Ω_c, ω) coupling, the $\pi^3\pi$ configuration will generate eight surfaces: five correlating with the $\mathrm{I}(^2\mathrm{P}_{3/2})$ limit and three with the $\mathrm{I}(^2\mathrm{P}_{1/2})$ limit. The $\pi^3\sigma$ configuration will generate six surfaces, with three correlating with each of the iodine-atom limits. Therefore in either configuration there are multitudinous possibilities for potential energy surface interactions.

The Hamiltonian appropriate to the photodissociation of ICN is

$$H = H_e + \mathsf{T} + H_{rel}, \tag{2}$$

where H_e is the electronic Hamiltonian, T is the nuclear kinetic-energy operation (incorporating vibration and rotation along with the radial terms), and H_{rel} is the relativistic part that incorporates the effects of spin–orbit interactions, hyperfine coupling and spin–spin interactions. The hyperfine and spin–spin terms are neglected in most treatments, leading to the simplification $H_{rel} \simeq H_{so}$, where H_{so} is the spin–orbit Hamiltonian. Here H_e describes the electrostatic and exchange forces between the fragments and is usually parametrized in terms of the adiabatic Born–Oppenheimer potential-energy surfaces (ABO).

One constituent part of T is a term

$$\frac{1}{2\mu R^2}\, l^2, \tag{3}$$

where

$$\mu = \frac{M_I(M_C + M_N)}{(M_I + M_C + M_N)}, \tag{4}$$

R is the I–CN centre-of-mass separation, and l describes the orbital angular momentum of the fragments about the centre of mass. For the general case where J_{parent} (the rotational angular momentum of the parent) is non-zero, this term gives rise to Coriolis coupling between potential-energy surfaces with the same electron spin multiplicity. We note, following Freed and co-workers [18], that, while the magnitude of the Coriolis coupling varies proportionally to R^{-2}, the attraction terms in H_e vary

asymptotically with high inverse powers of R. At some critical seam of internuclear separation R_{critical} and beyond, the Coriolis forces will become equal to, and exceed, the separation between the ABO potential-energy surfaces. Equally, Coriolis coupling can be neglected for $R \leqslant R_{\text{critical}}$. Physically, R_{critical} represents a boundary in the region of internuclear separation, dubbed the 'recoupling region' by Freed and co-workers. At this boundary and beyond, it is no longer appropriate to describe the system in the molecular-fixed basis, and one must consider a basis set comprised of linear combinations of the asymptotic fragment states, with the qualifier that, as R approaches infinity, the Coriolis forces decay to zero.

Spin–orbit coupling is present for all values of R. In the asymptotic limit, in the space-fixed basis, this coupling is diagonal, but becomes non-diagonal in the molecule-fixed frame. To date, this switch has been treated perturbatively, but, with our system yielding the iodine atom with a spin–orbit splitting of 7603 cm^{-1} [32], this treatment may not be appropriate. In general, spin–orbit interactions will couple surfaces of different spin multiplicity, i.e. $^1\Sigma^+$ and $^3\Pi$. More subtle perhaps is the possibility of coupling the different projection states of surfaces of $^3\Sigma$ and $^3\Pi$ character, i.e. states of different Ω. Joswig *et al.* [21] have already implicated the latter effect in the course of formulating an explanation for the non-statistical population of the spin–rotation doublets seen for this type of dissociation [33–35]. Consider the situation where $J_{\text{parent}} = 0$. Joswig *et al.* identify a component term of the spin–orbit Hamiltonian, namely

$$\frac{\boldsymbol{l}^2}{2\mu R^2}, \tag{5}$$

where

$$\boldsymbol{l} = -(\boldsymbol{N} + \boldsymbol{J}_{12}), \tag{6}$$

with $\boldsymbol{N}$ the CN nuclear angular momentum and $\boldsymbol{J}_{12}$ describing the coupling of the CN lone electron spin $\boldsymbol{s}$ with the electronic angular momentum $\boldsymbol{j}$ of the iodine atom:

$$\boldsymbol{J}_{12} = \boldsymbol{j} + \boldsymbol{s}. \tag{7}$$

Substituting (6) into (5), a coupling term of the form

$$\frac{\boldsymbol{N} \cdot \boldsymbol{J}_{12}}{\mu R^2} \tag{8}$$

emerges. This constitutes a force directed *out of the plane of scattering*, and its effect is to couple states $|M_{12}, M_N\rangle$ with states $|M_{12} \pm 1, M_N \mp 1\rangle$, where M_{12} and M_N are the projections of $\boldsymbol{J}_{12}$ and $\boldsymbol{N}$ on the quantization axis.

The above has concentrated on Coriolis effects caused by molecular rotation. However, as Vigué has pointed out to us [36], electrostatic coupling induced by molecular bending may also couple these states. This force is likely to be of an even larger magnitude.

We see that a variety of possible mechanisms exist to couple the ABO surfaces in the dissociation of ICN at 249 nm, following our conceptual generalization of the theory of Freed and co-workers [18]. This work was developed originally for diatomics, and, while we feel that the precepts are perfectly acceptable for extension to polyatomic molecules, we also note (regrettably) that the extension, even to a triatomic, involves formidable complications. Even with the advent of *ab initio* potential-energy surfaces for this system [37], there are additional complications of axis-switching [38–41], and

questions remain regarding the treatment of the iodine-atom spin–orbit coupling. We feel, however, that the results we have discussed here and elsewhere will require just such a progression of theory to provide a valid global explanation.

The observation of orientation of the fragments and its variation with fragment rotation is itself remarkable, since the initial photon absorption only carries one unit of angular-momentum helicity into a system having many quanta of rotation. Vigué *et al.* [14] and Dixon [15] have identified the phenomenon of vibronic angular-momentum amplification in dissociating systems. This has allowed us to understand the origins of large imbalances of spatial angular momentum in the fragments. What remains as a challenge to the theorists is to provide a detailed understanding of asymptotic fragment vector properties in systems exhibiting non-adiabatic dissociation.

5. Conclusion

Sub-Doppler probing of the CN ($X^2\Sigma^+$, $v = 2$) fragments from the photodissociation of ICN at 249 nm, using circularly polarized light, has produced evidence for quantum-threshold interference effects affecting the M_J distributions of the CN photofragment. This evidence, when cross-correlated with the results of previous experimental studies, provides conclusive proof for the presence of non-adiabatic interactions. The physical basis for explaining these observations rests on the breakdown of the Born–Oppenheimer approximation in systems evolving to asymptotic states possessing non-vanishing electronic angular momentum.

J.F.B. thanks SERC (U.K.) for support under the SERC/NATO postdoctoral fellowship scheme. E.H. thanks the Deutsche Forschungsgemeinschaft for a postdoctoral fellowship. This work was supported by NSF-PHY-88-05603.

References

[1] Simons, J. P., 1971, *Spectroscopy and Photochemistry* (Wiley-Interscience).
[2] Hall, G. E., and Houston, P. L., 1989, *A. Rev. phys. Chem.*, **40**, 375.
[3] Special issue, 1986, *J. chem. Soc. Faraday Trans. 2*, **82.**
[4] Shapiro, M., and Brumer, P., 1989, *J. chem. Phys.*, **90**, 6179.
[5] Tannor, D. J., and Rice, S. A., 1988, *Evolution of Size Effects in Chemical Dynamics*, edited by I. Prigogine and S. A. Rice (Wiley), p. 429.
[6] Vasyutinskii, O. S., 1980, *Soviet Phys. JETP Lett.*, **31**, 429.
[7] Vasyutinskii, O. S., 1981, *Opt. Spectrosc. (U.S.S.R.)*, **51**, 124.
[8] Heinzmann, U., 1985, *Applications of Circularly Polarized Radiation Using Synchrotron and Ordinary Sources*, edited by F. Allen and C. Bustamente (Plenum), pp. 1–11.
[9] Kessler, J., 1976, *Polarized Electrons* (Springer), Chap. 5.
[10] Cherepkov, N. A., 1983, *Adv. atom. molec. Phys.*, **19**, 395.
[11] Hasselbrink, E., Waldeck, J. R., and Zare, R. N., 1988, *Chem. Phys.*, **126**, 191.
[12] Black, J. F., Waldeck, J. R., and Zare, R. N., 1990, *J. chem. Phys.*, **92**, 3519.
[13] Black, J. F., Waldeck, J. R., Hasselbrink, E., and Zare, R. N., 1989, *J. chem. Soc. Faraday Trans. 2*, **85**, 1044.
[14] Vigué, J., Girard, B., Gouédard, G., and Billy, N., 1989, *Phys. Rev. Lett.*, **62**, 1358.
[15] Dixon, R. N., 1989, *Molec. Phys.*, **68**, 263.
[16] Band, Y. B., Freed, K. F., and Kouri, D. J., 1981, *Chem. Phys. Lett.*, **79**, 233.
[17] Band, Y. B., Freed, K. F., and Kouri, D. J., 1981, *Chem. Phys. Lett.*, **79**, 238.
[18] Williams, C. J., Freed, K. F., Singer, S. J., and Band, Y. B., 1986, *J. chem. Soc. Faraday Trans. 2*, **82**, 51, and references therein.
[19] Black, J. F., Waldeck, J. R., and Zare, R. N., 1989, *J. chem. Soc. Farad. Trans. 2*, **85**, 1312.
[20] O'Halloran, M. A., Joswig, H., and Zare, R. N., 1987, *J. chem. Phys.*, **87**, 303.

[21] JOSWIG, H., O'HALLORAN, M. A., ZARE, R. N., and CHILD, M. S., 1986, *J. chem. Soc. Faraday Trans. 2*, **82**, 79.
[22] HERZBERG, G., 1950, *Molecular Spectra and Molecular Structure* I. *Spectra of Diatomic Molecules* (Van Nostrand Reinhold).
[23] WEINARD, J., 1955, *Ann. Astrophys.*, **18**, 334.
[24] BROCKLEHURST, B., HERBERT, G. R., INNANEN, S. H., SEEL, R. M., and NICHOLS, R. W., 1972, *Identification Atlas of Molecular Spectra. 9. The CN* $B^2\Sigma^+$–$X^2\Sigma^+$ *Violet System* (York University Centre for Research in Experimental Space Science).
[25] ENGLEMAN, R. JR., 1974, *J. molec. Spectrosc.*, **49**, 106.
[26] CERNY, D., BACIS, R., GUELACHVILI, G., and ROUX, F., 1978, *J. molec. Spectrosc.*, **73**, 154.
[27] ITO, H., OZAKI, Y., SUZUKI, K., KONDOW, T., and KUCHITSU, K., 1988, *J. molec. Spectrosc.*, **127**, 283.
[28] WALDECK, J. R., BLACK, J. F., and ZARE, R. N. (unpublished work).
[29] WALDECK, J. R., 1989, Ph.D. thesis, Stanford University.
[30] KING, G. W., and RICHARDSON, A. W., 1966, *J. molec. Spectrosc.*, **21**, 339.
[31] RABALAIS, J. W., MCDONALD, J. M., SCHERR, V., and MCGLYNN, S. P., 1971, *Chem. Rev.*, **71**, 73.
[32] MOORE, C. E., 1958, *Atomic Energy Levels*, Vol. 3 reissue 1971 (United States Government Printing Office).
[33] SHOKOOHI, F., HAY, S., and WITTIG, C., 1984, *Chem. Phys. Lett.*, **110**, 1.
[34] NADLER, I., MAHGEREFTEH, D., REISLER, H., and WITTIG, C., 1985, *J. chem. Phys.*, **82**, 3885.
[35] PAUL, A., FINK, W. H., and JACKSON, W. M., 1988, *Chem. Phys. Lett.*, **153**, 121.
[36] VIGUÉ, J., 1990 (private communication).
[37] MOROKUMA, K., and YAHUSHITA, S., 1990 (private communication).
[38] BAND, Y. B., and FREED, K. F., 1975, *J. chem. Phys.*, **63**, 3382.
[39] MORSE, M. D., FREED, K. F., and BAND, Y. B., 1979, *J. chem. Phys.*, **70**, 3604.
[40] MORSE, M. D., FREED, K. F., and BAND, Y. B., 1979, *J. chem. Phys.*, **70**, 3620.
[41] MORSE, M. D., and FREED, K. F., 1981, *J. chem. Phys.*, **74**, 4395.